cw instability and steady-state pulses in a ring laser with intracavity parametric amplification

M. B. Pande and S. Dutta Gupta
School of Physics, University of Hyderabad, Hyderabad 500 134, India
(Received 2 July 1992)

A homogeneously broadened two-level ring laser with an intracavity parametric amplifier is studied. The presence of the parametric amplifier is shown to lead to two distinct nontrivial cw solutions compared to the one in its absence. The conditions for the stability of these cw solutions are obtained. It is shown that in the context of the resonant modes one cw solution is always phase stable, whereas the other is always phase unstable. For pump parameters beyond a critical value (the second threshold), both these cw solutions become amplitude unstable, and self-pulsing can set in. The shape and the velocity of these pulses are evaluated numerically. It is shown that two distinct types of steady-state pulses beyond the second laser threshold are possible due to the phase sensitivity introduced by the parametric amplifier. This is in sharp contrast to the case without the parametric amplifier, where only Risken-Nummedal pulses [see H. Risken and K. Nummedal, J. Appl. Phys. **39**, 4662 (1968)] are possible. It is shown that the parametric amplifier can lead to the narrowing or broadening of the Risken-Nummedal pulses. Moreover, it is shown that the ring laser with or without the parametric amplifier allows for a pulsed solution distinct from the above-mentioned one, which, however, turns out to be unstable.

PACS number(s): 42.60.Mi, 42.65.Re

I. INTRODUCTION

It is well known that in the context of a single-mode theory the introduction of a phase-sensitive element like a parametric amplifier (PA) or phase-conjugate mirror can drastically affect the dynamics of a ring laser [1–3]. In fact, so far as the regular (chaotic [4]) motion is concerned, the insertion of the phase-sensitive element in the cavity leads to the birth of additional fixed points (strange attractors). Moreover, the character of the fixed points or the strange attractor (in terms of realization in the long run) depends crucially on the parameters of the phase-sensitive element. For example, for a PA, it depends on the second-order susceptibility $\chi^{(2)}$ of the PA crystal and the strength of its pumping. It is of interest to investigate the effects, for example, of a PA when one deviates from the single-mode approximation. A multimode analysis [5] would mean the retention of the spatial dependence of the concerned variables. Risken and Nummedal (RN) have studied the instabilities [6,7] (hereafter referred to as the RN instability) in a ring laser retaining all the modes of the structure. They have shown that a stable cw solution exists below the second laser threshold [6]. Above the second threshold the cw solution becomes unstable and the realized states of the system are pulses (hereafter referred to as RN pulses [7]) moving with a characteristic velocity. In this paper we address the question of how the introduction of the PA affects the RN instability. In all our calculations we closely follow Ref. [7]. We show that, like in the single-mode case the presence of the PA leads to additional fixed points (cw states) below the second second threshold. In fact there are now two "second thresholds" so far as the amplitude stability is concerned. Among the pair of cw states, one becomes amplitude unstable beyond the first second threshold, whereas both are unstable beyond the second second threshold. In the regime where the cw states are unstable one has self-pulsing with two distinct types of pulses, one narrower and the other broader compared to the RN pulses. Thus one can manipulate the pulse width with the help of a PA. For fixed system parameters one of the above two pulsed solutions is stable. Note that the laser equations allow for nonsteady breathing solutions [8]. However, in this paper we concentrate only on the steady-state pulses and we do not consider breathing solutions. Another pertinent question which we address in this paper is the following: Are the RN pulses the only steady-state pulsed solutions allowed by the equations and the boundary conditions? We show that other steady-state pulsed solutions can exist. However, they are not physical since they turn out to be unstable in the realistic parameter space. Nevertheless, the existence of such solutions keeps the question of other types of stable solutions open.

The organization of the paper is as follows. In Sec. II, we discuss the model and present the basic equations. In Sec. III, we obtain the cw solutions and present the results pertaining to the linear stability of these solutions. In Sec. IV, we study the simplified equations for the steady-state pulses and numerically integrate them to obtain the pulse shape and the characteristic velocity. In the same section we comment on the stability of the pulsed solutions. Finally, in Sec. V, we conclude the paper.

II. THE MODEL AND THE BASIC EQUATIONS

Consider a ring laser with one cavity mode in resonance with the atomic frequency ω_0. We assume the presence of a $\chi^{(2)}$ material in the cavity. The nonlinear crystal is pumped at twice the atomic frequency. The nonlinear material will convert the pumping radiation at

$2\omega_0$ into radiation at ω_0 [1]. The dynamics of the atoms and the field in the cavity with the PA in the rotating-wave approximation can be described by the equations

$$\dot{P}+\gamma_\perp P=\gamma_\perp E\sigma \ , \tag{2.1}$$

$$\dot{\sigma}+\gamma_\parallel\sigma=\gamma_\parallel[\lambda+1-(\lambda/2)(E^*P+EP^*)] \ , \tag{2.2}$$

$$c\frac{\partial E}{\partial x}+\dot{E}+\kappa E=\kappa P+GE^* \ , \tag{2.3}$$

where P, σ, and E are the polarization, inversion, and the electric field, respectively; $\gamma_\parallel,\gamma_\perp$ are the longitudinal and transverse decay rates; κ is the cavity decay rate; λ is the pump parameter. Note that the insertion of the PA leads to an additional term in the equation for the electric field [the last term in Eq. (2.3)]. The complex parameter G ($=ge^{i\theta}$, g and θ are the modulus and argument of G) in Eq. (2.3) is proportional to $\chi^{(2)}$ of the nonlinear crystal and the amplitude of radiation pumping the nonlinear crystal. In Eq. (2.1)–(2.3) the overdot represents a time derivative and all the variables E, P, and σ are normalized to the corresponding steady-state values in the absence of the PA (i.e., when $G=0$).

In a ring cavity Eqs. (2.1)–(2.3) have to be supplemented by periodic boundary conditions which can be written as follows [7]:

$$\begin{aligned} &E(x+L,t)=E(x,t) \ , \\ &P(x+L,t)=P(x,t) \ , \\ &\sigma(x+L,t)=\sigma(x,t) \ , \end{aligned} \tag{2.4}$$

where L is the cavity length. We now make use of the transformations

$$E(x,t)=e(x,t)e^{i[\varphi(x,t)+\theta/2]} \ , \tag{2.5}$$

$$P(x,t)=p(x,t)e^{i[\psi(x,t)+\theta/2]} \ , \tag{2.6}$$

with e, p, φ, and ψ real in Eqs. (2.1)–(2.3). The resulting equations do not contain the argument θ of the nonlinearity parameter G and can be written as

$$\dot{p}+\gamma_\perp p=\gamma_\perp e\sigma\cos(\varphi-\psi) \ , \tag{2.7}$$

$$\dot{\sigma}+\gamma_\parallel\sigma=\gamma_\parallel[\lambda+1-\lambda ep\cos(\varphi-\psi)] \ , \tag{2.8}$$

$$\dot{e}+c\frac{\partial e}{\partial x}+\kappa e=\kappa p\cos(\varphi-\psi)+eg\cos 2\varphi \ , \tag{2.9}$$

$$p\dot{\psi}=\gamma_\perp e\sigma\sin(\varphi-\psi) \ , \tag{2.10}$$

$$ce\frac{\partial\varphi}{\partial x}+e\dot{\varphi}=-\kappa p\sin(\varphi-\psi)-eg\sin 2\varphi \ . \tag{2.11}$$

It is clear from Eqs. (2.5) and (2.6) and the absence of θ in Eqs. (2.7)–(2.11) that the phase of the nonlinearity parameter leads only to a rotation of the complex amplitudes E and P in the complex plane, and does not otherwise affect the dynamics of the system.

Note that in absence of the PA ($g=0$) the set of Eqs. (2.7)–(2.11) reduces to the set investigated by Risken and Nummedal [7]. The introduction of the PA leads to extra terms [see Eqs. (2.9) and (2.11)] which depend crucially on the phase of the electric field.

III. cw SOLUTIONS AND THEIR LINEAR STABILITY

In this section we obtain the cw solutions (for $\partial/\partial t=\partial/\partial x=0$) for the system of Eqs. (2.7)–(2.11), and investigate the linear stability of these solutions. In presence of the PA, there exists a pair of cw solutions (denoted by overbars) given by

$$\bar{\sigma}=1+q\frac{g}{\kappa} \ , \tag{3.1}$$

$$\bar{e}^2=[1+(1-\bar{\sigma})/\lambda]/\bar{\sigma} \ , \tag{3.2}$$

$$\bar{p}^2=\bar{\sigma}[1+(1-\bar{\sigma})/\lambda] \ , \tag{3.3}$$

where q can take value ±1. The values of the phases $\bar{\varphi}$ and $\bar{\psi}$ corresponding to the cw states are given by

$$\bar{\varphi}=\bar{\psi}=\begin{cases}0 \ , & \text{for } q=-1 \ , \\ \pi/2 \ , & \text{for } q=+1 \ .\end{cases} \tag{3.4}$$

Note that for $g=0$, both these solutions become identical and one recovers the cw state $\bar{e}=\bar{p}=\bar{\sigma}=1$ and $\bar{\varphi}=\bar{\psi}$ = constant of the ring laser in the absence of the PA. In order to investigate the linear stability of the solutions given by Eqs. (3.1)–(3.4) we adopt the standard technique of perturbations around these cw states [7]. The linearized equations for the perturbations δp, $\delta\sigma$, δe, $\delta\varphi$, and $\delta\psi$ can be written as

$$\delta\dot{p}+\gamma_\perp\delta p=\gamma_\perp\bar{e}\delta\sigma+\gamma_\perp\bar{\sigma}\delta e \ , \tag{3.5}$$

$$\delta\dot{\sigma}+\gamma_\parallel\delta\sigma=\gamma_\parallel[-\lambda\bar{e}\delta p-\lambda\bar{p}\delta e] \ , \tag{3.6}$$

$$\delta\dot{e}+c\frac{\partial}{\partial x}(\delta e)+\kappa\delta e=\kappa\delta p-qg\delta e \ , \tag{3.7}$$

$$\bar{p}\delta\dot{\psi}=\gamma_\perp\bar{e}\bar{\sigma}(\delta\varphi-\delta\psi) \ , \tag{3.8}$$

$$\bar{e}\delta\dot{\varphi}+c\bar{e}\frac{\partial}{\partial x}(\delta\varphi)=-\kappa\bar{p}(\delta\varphi-\delta\psi)+q\bar{e}g2\delta\varphi \ . \tag{3.9}$$

It can be seen from Eqs. (3.5)–(3.9) that even in the presence of the PA the equations for amplitude perturbations δp, $\delta\sigma$, and δe are decoupled from those for phase perturbations $\delta\psi$ and $\delta\varphi$. As in Ref. [7], we make the ansatz that all the perturbations vary as

$$\delta p,\delta\sigma,\delta e,\delta\psi,\delta\varphi\sim\exp[i\alpha(L/c)x+\beta t]+\text{c.c.} \ , \tag{3.10}$$

where α and β are constants. For infinite medium α can take any value from $-\infty$ to $+\infty$, whereas for a cavity α can take only discrete values

$$\alpha_n=2\pi\frac{c}{L}n \ , \quad n=0,\pm1,\ldots \ . \tag{3.11}$$

The use of the ansatz (3.10) in Eqs. (3.5)–(3.9) leads to a set of homogeneous linear algebraic equations with respect to the moduli of the perturbations δp, $\delta\sigma$, δe, $\delta\varphi$, and $\delta\psi$. The condition of nontriviality of the solution of this set yields the following characteristic equations for the stability of the amplitudes and phases, respectively:

$$\tilde{\beta}^3+a_1\tilde{\beta}^2+a_2\tilde{\beta}+a_3=0 \ , \tag{3.12}$$

$$\tilde{\beta}^2+b_1\tilde{\beta}+b_2=0 \ , \tag{3.13}$$

where

$$a_1 = i\tilde{\alpha} + 1 + \tilde{\gamma}_\parallel + \tilde{\kappa} + q\tilde{g} \ ,$$
$$a_2 = \tilde{\gamma}_\parallel(\tilde{\kappa} + q\tilde{g} + 1) + i\tilde{\alpha}(1 + \tilde{\gamma}_\parallel) + \lambda\tilde{\gamma}_\parallel\bar{e}^2 \ , \quad (3.14)$$
$$a_3 = i\tilde{\alpha}\tilde{\gamma}_\parallel(1 + \lambda\bar{e}^2) + 2\lambda\tilde{\gamma}_\parallel\tilde{\kappa}\bar{e}^2(1 + q\tilde{g}/\tilde{\kappa}) \ ,$$

and

$$b_1 = i\tilde{\alpha} + \tilde{\kappa} + 1 - q\tilde{g} \ ,$$
$$b_2 = i\tilde{\alpha} - 2q\tilde{g} \ . \quad (3.15)$$

In Eqs. (3.12)–(3.15) the tilde denotes normalization with respect to the transverse decay rate $\gamma_\perp$ (for example, $\tilde{\gamma}_\parallel = \gamma_\parallel/\gamma_\perp$). We now look for the roots of $\tilde{\beta}$ for real $\tilde{\alpha}$ corresponding to the Eqs. (3.12) and (3.13). Instability of the amplitudes (phases) is heralded by the existence of a positive real part of the root of Eq. (3.12) [Eq. (3.13)]. The condition for amplitude instability can be written as

$$\lambda > \lambda_{cr} = q\frac{\tilde{g}}{\tilde{\kappa}} + \left[1 + q\frac{\tilde{g}}{\tilde{\kappa}}\right] \times [4 + 3\tilde{\gamma}_\parallel + 2(4 + 6\tilde{\gamma}_\parallel + 2\tilde{\gamma}_\parallel^2)^{1/2}] \ . \quad (3.16)$$

Note that λ_{cr} now has two values since q can take values ± 1 corresponding to the pair of cw solutions. Let us denote the value of λ_{cr} by λ_{cr-} (λ_{cr+}) for $q = -1$ ($+1$). It is clear from Eq. (3.16) that $\lambda_{cr-} < \lambda_{cr+}$. Thus for $\lambda < \lambda_{cr-}$, both the cw solutions are amplitude stable. For $\lambda_{cr-} < \lambda < \lambda_{cr+}$ the solution corresponding to $q = +1$ is the only (amplitude) stable solution. For $\lambda > \lambda_{cr+}$ both the solutions become unstable. Hence the solution corresponding to $q = -1$ is more prone to cw instability (so far as the amplitudes are concerned). Thus, the ring laser with the PA allows for a double second threshold $\lambda_{cr\pm}$ so far as the amplitudes are concerned, below the least of which the system may support two distinct cw states. The finally realized state will depend on the phase stability of these solutions and the initial conditions.

We now turn to phase instability. In absence of the PA, the phases are known to be marginally stable. The situation here is altogether different since the two solutions behave differently in the context of phase instability. Since Eq. (3.13) is a quadratic, it can be directly solved for the values of $\tilde{\beta}$. However, we only look for the boundary of the stable and unstable regions in the parameter space, i.e., we look for real solutions for $\mathrm{Im}(\beta)$ setting $\mathrm{Re}(\beta) = 0$. This leads to the equation

$$(\mathrm{Im}\beta)^2 = \frac{2q\tilde{g}}{\tilde{\kappa} - q\tilde{g}} \ . \quad (3.17)$$

It is clear from Eq. (3.17) that for $q = -1$, real solutions for $\mathrm{Im}\beta$ are not possible and hence the cw solution corresponding to $q = -1$ are always phase stable. The $q = +1$ solutions which are less prone to amplitude instability can suffer phase instability. Note that generally $\tilde{g} < \tilde{\kappa}$, and for $q = +1$ the modes close to the resonant one are always phase unstable. The solutions for $\mathrm{Im}(\beta)$ corresponding to the boundary of the stable domain can be obtained from Eq. (3.17) by setting $q = +1$. The range of values of $\tilde{\alpha}$ corresponding to the unstable domain can also be calculated. However, we do not present those results here.

The analytical results cited above were corroborated by direct numerical solution of the Eqs. (3.12) and (3.13). Calculations were carried out for $\tilde{\gamma}_\parallel = 0.5$ and for two different values of the normalized cavity damping parameter $\tilde{\kappa}$, namely, $\tilde{\kappa} = 0.1$ and 3. The value of the pump parameter λ was chosen to be 15. For $\tilde{\kappa} = 0.1$ ($\tilde{\kappa} = 3.0$) $\tilde{g}/\tilde{\kappa}$ was chosen to be 0.5 (0.09). Note that for $\tilde{\gamma}_\parallel = 0.5$, $\tilde{\kappa} = 0.1$, and $\tilde{g}/\tilde{\kappa} = 0.5$, $\lambda_{cr-} = 4.98$ and $\lambda_{cr+} = 16.955$. Thus this choice of parameters for $\lambda = 15$, correspond to the case when only $q = -1$ solution can be amplitude unstable. The other choice (i.e., $\tilde{\kappa} = 3.0$, $\lambda = 15$, and $\tilde{g}/\tilde{\kappa} = 0.09$) corresponds to the case when both the cw solutions can show amplitude instability. The results are

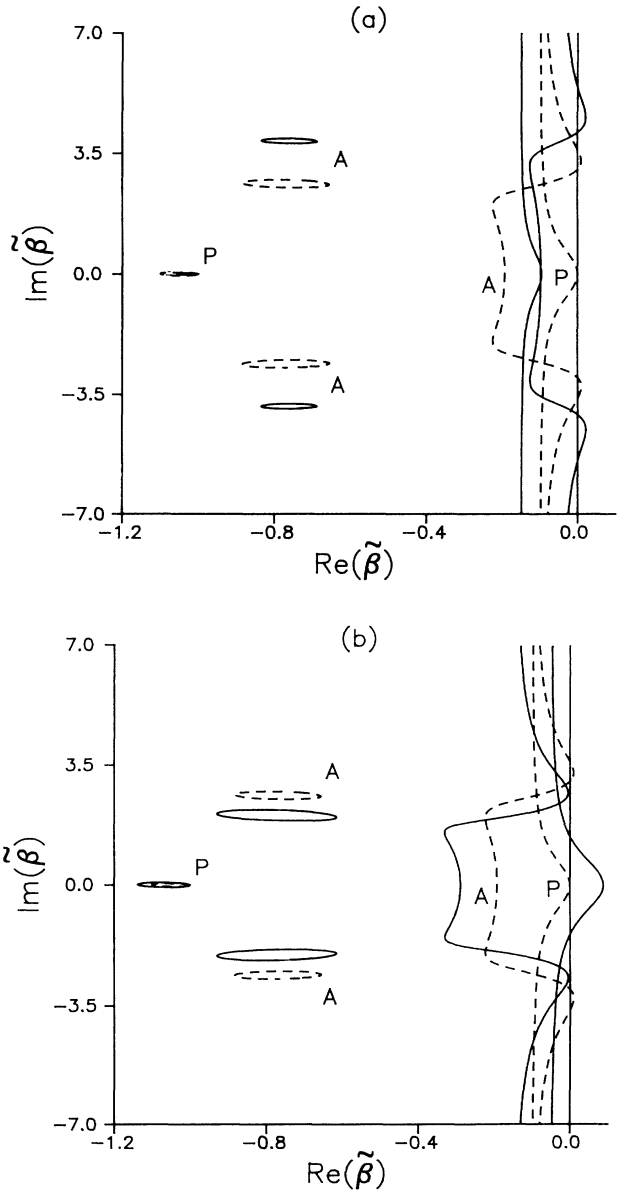

FIG. 1. $\mathrm{Im}(\tilde{\beta})$ as a function of $\mathrm{Re}(\tilde{\beta})$ with the parameter $\tilde{\alpha}$ varying from $-\infty$ to $+\infty$. The solid curves are for (a) $q = -1$, $\tilde{g}/\tilde{\kappa} = 0.5$ and (b) $q = +1$, $\tilde{g}/\tilde{\kappa} = 0.5$. The dashed curves are for $g = 0$ which corresponds to the case when the PA is absent. Other parameters are $\lambda = 15$, $\gamma_\parallel = 0.5$, $\tilde{\kappa} = 0.1$. Curves marked by A (P) correspond to the amplitudes (phases).

shown in Figs. 1 and 2, where we have plotted $\mathrm{Im}(\tilde{\beta})$ as a function of $\mathrm{Re}(\tilde{\beta})$ as $\tilde{\alpha}$ is scanned from $-\infty$ to $+\infty$. We have reproduced the results of Ref. [7] on all these curves for the sake of comparison. Figures 1(a) and 2(a) [1(b) and 2(b)] show the dependence for $q=-1$ ($q=+1$). On these figures curves marked A (P) are for amplitudes (phases). It can be seen from Fig. 1(a) that the $q=-1$ solution shows enhanced amplitude instability. The phase of these solutions which was marginally stable in absence of the PA now become stable for all values of $\tilde{\alpha}$. Moreover, the domain of instability shifts away from the central resonant mode. The other solution for $q=+1$ shows a different tendency [see Fig. 1(b)]. $q=+1$ solutions for the said parameter values do not exhibit amplitude instability. But the phases of these solutions can become unstable for $\tilde{\alpha}$ close to zero. Thus the on-resonant modes for $q=+1$ always show phase instability. A comparison of Figs. 1(a) and 1(b) reveals that the mechanism of instability in the two solutions $q=-1$ and $q=+1$ are of different nature. $q=-1$ solutions can become unstable due to the instability of the off-resonant modes, whereas for $q=+1$ the instability is basically due to the phase fluctuations of the modes close to the resonant one. Though over and above phase instability $q=+1$ solutions can show amplitude instability of the off-resonant modes for sufficiently large pumping. Similar features are observed for the other set of parameters [see Figs. 2(a) and 2(b)]. In contrast to Fig. 1(b) we now have the amplitude instability of the off-resonant modes for $q=+1$ [Fig. 2(b)]. However, compared to the case when the PA is absent, the domains of instability move closer to the resonant mode.

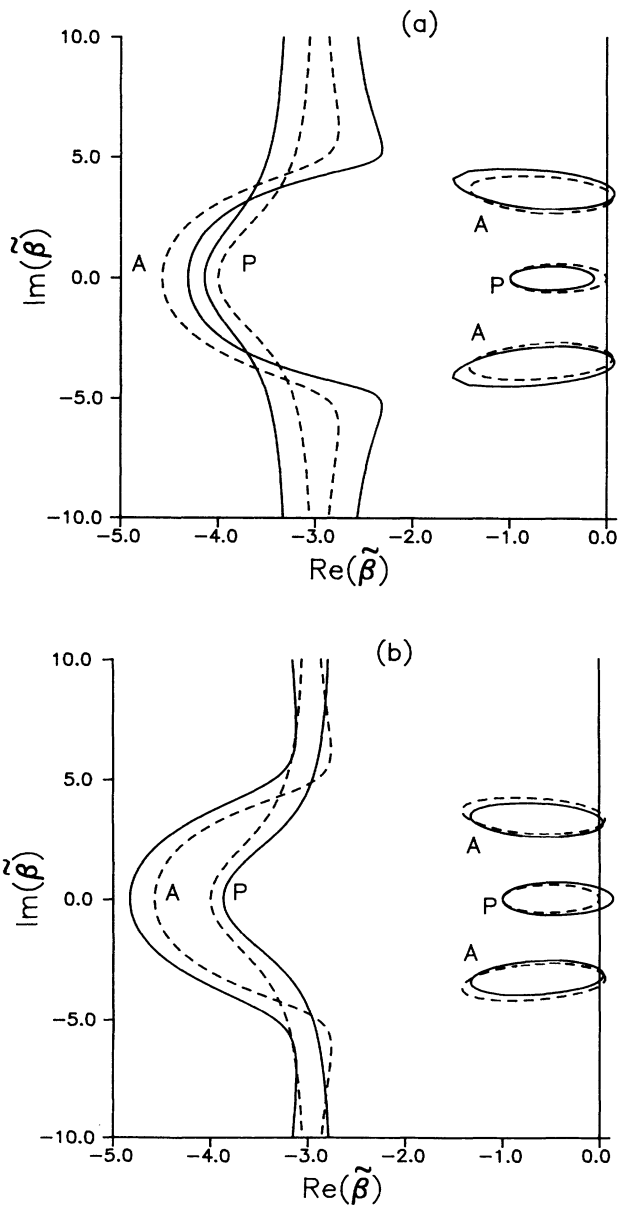

FIG. 2. Same as in Fig. 1 except that now $\tilde{\kappa}=3.0$ and the solid curves are for $\tilde{g}/\tilde{\kappa}=0.09$.

IV. STEADY-STATE PULSES IN THE PRESENCE OF THE PARAMETRIC AMPLIFIER

In this section we concentrate on the parameter range in which the cw solutions discussed earlier become unstable. Evidently the temporal growth of the amplitudes and the phases in the framework of a linear theory renders them to be large enough leading to a breakdown of the linearization approximation and an exact analysis is called for. In our analysis we follow Ref. [7] and study the truncated system for only the amplitudes. The justification for this simplified approach in the context of the present problem will be given later on the basis of numerical integration of the full set of Eqs. (2.7)–(2.11). We look for steady-state pulses of Eqs. (2.7)–(2.9) moving with a velocity v. Introducing the dimensionless coordinate ζ as

$$\zeta=(t-x/v)/(L/v) \tag{4.1}$$

the equations for the steady-state pulses can be written as follows:

$$\frac{dp}{d\zeta}=(2\pi/\tilde{\alpha}')(e\sigma-p)\ , \tag{4.2}$$

$$\frac{d\sigma}{d\zeta}=(2\pi\tilde{\gamma}_{\parallel}/\tilde{\alpha}')(\lambda+1-\lambda ep-\sigma)\ , \tag{4.3}$$

$$\frac{de}{d\zeta}=(2\pi/\tilde{\epsilon}\tilde{\alpha}')\{p-[1+q(\tilde{g}/\tilde{\kappa})]e\}\ . \tag{4.4}$$

In Eqs. (4.2)–(4.4),

$$\tilde{\alpha}'=2\pi(v/L)/\gamma_{\perp}\ , \tag{4.5}$$

and the parameter $\tilde{\epsilon}$ defined as

$$\tilde{\epsilon}=(1-c/v)/\tilde{\kappa} \tag{4.6}$$

determines the velocity of the pulses in an implicit form. In Eqs. (4.2)–(4.4) we have assumed that the phases φ and ψ of the electric field and polarization corresponding to the steady-state pulses are stable and for $q=-1$ ($q=+1$) they are given by $\varphi=\psi=0$ ($\varphi=\psi=\pi/2$). It will be shown later by numerical integration of the set of Eqs. (2.7)–(2.11) [9] that the phases corresponding to the stable $q=-1$ ($q=+1$) pulses indeed go to zero ($\pi/2$) in

the long-time limit. The set of Eqs. (4.2)–(4.4) has to be solved subject to the boundary conditions (2.4) which for the steady-state pulses read as follows:

$$p(\zeta+1)=p(\zeta)\,,$$
$$\sigma(\zeta+1)=\sigma(\zeta)\,, \tag{4.7}$$
$$e(\zeta+1)=e(\zeta)\,.$$

As in Ref. [7], we use the shooting technique to obtain the form of the steady-state pulsed solutions for $p(\zeta)$, $\sigma(\zeta)$, and $e(\zeta)$. We assume that at $\zeta=0$, $de/d\zeta=0$. This defines a relation between $e(0)$ and $p(0)$. Next, we guess the values of the parameters $\tilde{\epsilon}$, $e(0)$, and $\sigma(0)$. We integrate Eqs. (4.2)–(4.4) with these initial conditions to obtain the values of $p(1)$, $\sigma(1)$, and $e(1)$. Henceforth, the requirement that the boundary conditions [Eq. (4.7)] must be satisfied leads to three coupled nonlinear equations for the unknown parameter $\tilde{\epsilon}$ and the initial values $e(0)$ and $\sigma(0)$. These equations are solved using a modified Newton-Raphson technique. Finally with known parameter $\tilde{\epsilon}$ and the values of p, σ, and e at the left edge, the shape of the pulse is determined along the length of the cavity. The results of our numerical analysis are shown in Figs. 3 and 4 for two different values of the parameter $\tilde{\alpha}'$, namely, $\tilde{\alpha}'=3.0$ and $\tilde{\alpha}'=3.3$. In Fig. 3 we have shown two periods of e [Fig. 3(a)], p [Fig. 3(b)], and σ [Fig. 3(c)] as functions of ζ for $\tilde{\alpha}'=3.0$. We have plotted the results corresponding to both $q=-1$ and $q=+1$ pulses along with the RN pulse. It is clear from Fig. 3 that the $q=-1$ ($q=+1$) pulses are narrower (broader) with higher (lower) peak to crest ratio compared to the RN pulse. Thus the PA in the cavity leads to the possibility of controlling the pulse width. In

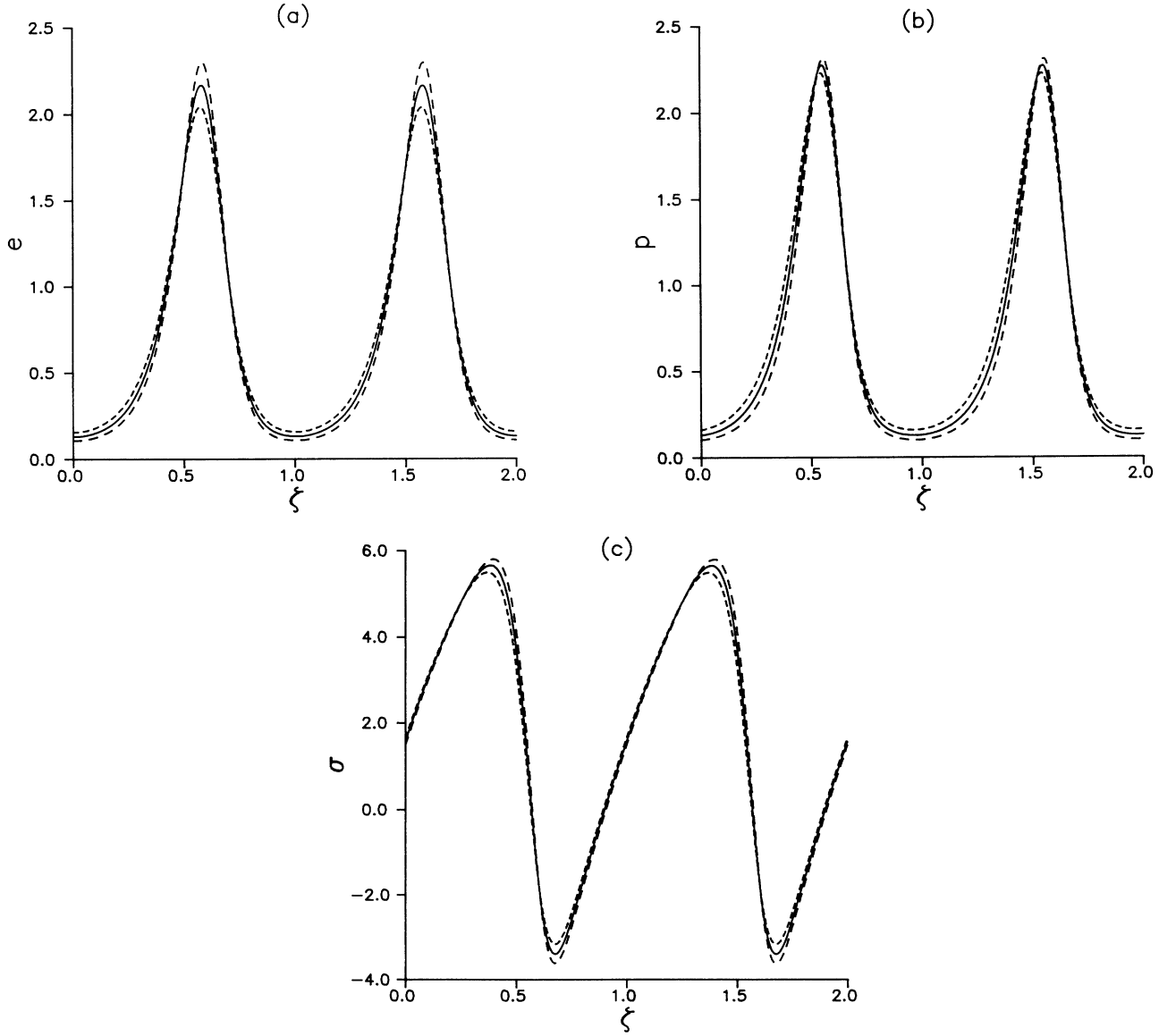

FIG. 3. Two periods of the steady-state fields (a) e, (b) p, and (c) σ as functions of the dimensionless coordinate ζ with (dashed curves) and without (solid curves) the PA for $\tilde{\alpha}'=3.0$. Curves with smaller (larger) dashes correspond to $q=+1$, $\tilde{g}/\tilde{\kappa}=0.04$ ($q=-1$, $\tilde{g}/\tilde{\kappa}=0.04$). Other parameters are $\lambda=15$, $\gamma_{\parallel}=0.5$.

particular it can contribute to pulse narrowing which may find practical applications. The other set of results for $\tilde{\alpha}'=3.3$ (see Fig. 4) reflect a similar pulse narrowing or broadening effect. We have also studied the dependence of the parameter $\tilde{\epsilon}$ on $\tilde{\alpha}'$ (see Fig. 5). Note that an increase in the velocity of the pulse leads to an increase in the values of $\tilde{\epsilon}$. It can be seen from Fig. 5 that $q=+1$ ($q=-1$) pulses are faster (slower) than the RN pulses. Thus the system with the PA allows for two different pulsed solutions, one narrower and the other broader. Moreover, the broader pulse propagates with a larger velocity. Some preliminary results on the stability of these pulses will be given at a later stage.

In order to assess the mode contents of these pulses we have expanded $e(\zeta)$ in a Fourier series using

$$e(\zeta)=\frac{a_0}{2}+\sum_{n=1}^{\infty} a_n \cos(2\pi n\zeta)+\sum_{n=1}^{\infty} b_n \sin(2\pi n\zeta) , \tag{4.8}$$

and looked at the first few Fourier coefficients. The results for $\lambda=15$, $\tilde{\gamma}_{\parallel}=0.5$, $\tilde{\alpha}'=3.3$ are shown in Figs. 6(a) and 6(b). Figure 6(a) [6(b)] shows the cosine [sine] components. It is clear from Fig. 6(a) that for $q=+1$ [$q=-1$], there is a slight increase [decrease] in the mean value ($a_0/2$) compared to the case of RN pulses. Moreover, so far as the other modes are concerned the oscillations of a_n around zero are less [more] pronounced for $q=+1$ [$q=-1$]. The same feature is observed for the coefficients b_n [see Fig. 6(b)]. Thus for $q=+1$ pulse, off-

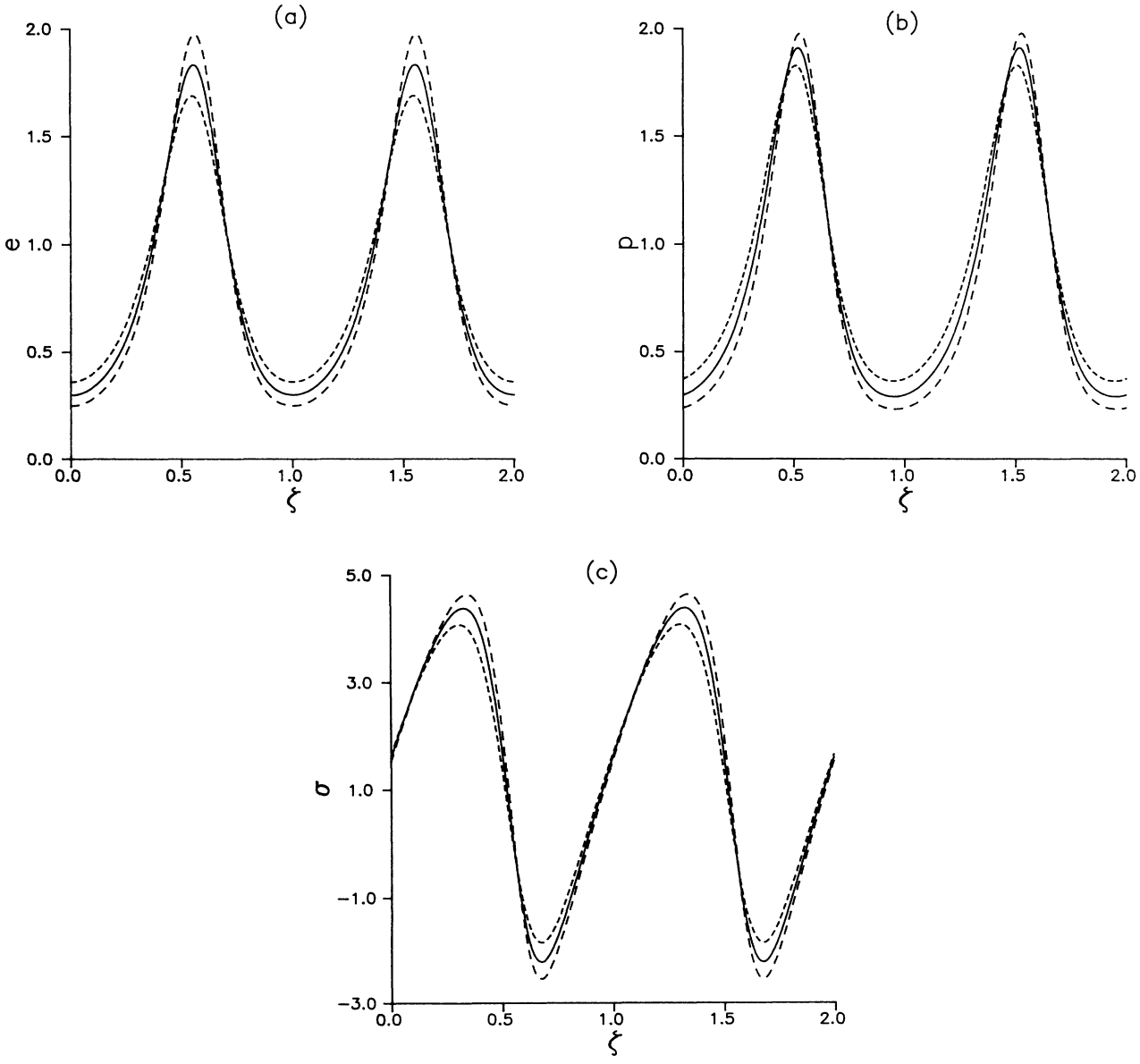

FIG. 4. Same as in Fig. 3 except for $\tilde{\alpha}'=3.3$.

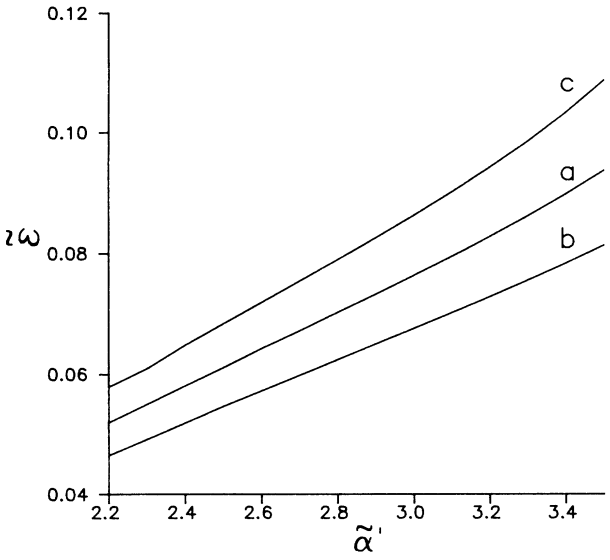

FIG. 5. Parameter $\tilde{\epsilon}$ as a function of $\tilde{\alpha}'$. Curve a is for the RN pulse ($g=0$), whereas curve b (c) is for $q=-1$ ($q=+1$) and $\tilde{g}/\tilde{\kappa}=0.04$. Other parameters are $\lambda=15$, $\gamma_{\parallel}=0.5$.

resonant modes are characterized by smaller amplitudes, and these pulses are more "symmetric" with respect to the peak or crest.

We now present some preliminary results on the stability of the pulses shown in Figs. 3 and 4. All our results and comments are based on the analysis of the full set of Eqs. (2.7)–(2.11) with the boundary conditions given by Eq. (2.4). We have noticed that the stability of the pulses depends on the normalized cavity damping parameter $\tilde{\kappa}$. However, the domain of stability in the $(\tilde{\alpha},\tilde{\kappa})$ plane for the $q=+1$ pulses does not overlap with the same for the $q=-1$ pulses. Thus for fixed system parameters only one of these two pulses can be stable. Thus a bistable operation between the two pulsed states in a ring laser with the PA seems to be impossible. We have found that for $\tilde{\alpha}'=3.0$ and $\tilde{\kappa}=1.3$ [which for $q=+1$, corresponds to $\tilde{\epsilon}=0.086\,32$, and $\tilde{\alpha}=(2\pi c/L)/\gamma_{\perp}=2.663$] only the $q=+1$ pulse is the stable one. We integrated the set of Eqs. (2.7)–(2.11) with initial conditions $e=e_s+i$, $p=p_s$, $\sigma=\sigma_s$, where e_s, p_s, and σ_s are the final steady-state pulse values corresponding to $q=+1$ in Fig. 3. The results are shown in Fig. 7. In Fig. 7(a) we have shown the temporal evolution of the maximum ($e_{\max}$) and minimum ($e_{\min}$) amplitudes of the electric field, whereas, in Fig. 7(b) the extremal values of φ and ψ are plotted. It is clear from Fig. 7(a) that in the long-time limit the extremal amplitudes reach their steady-state values defined by the stable $q=+1$ pulse. As was mentioned earlier, both the phases reach $\pi/2$ in the same limit thereby implying that the phases are stable [see Fig. 7(b)]. In order to check the stability of the $q=-1$ pulse corresponding to the same set of parmeters $\tilde{\alpha}'$, $\tilde{\kappa}$, and λ we integrated Eqs. (2.7)–(2.11) with an initial guess given by the pulse corresponding to $q=-1$ in Fig. 3. Note that since $\tilde{\epsilon}$ is different for the $q=-1$ pulse one has a different value of $\tilde{\alpha}$ ($\tilde{\alpha}=2.7361$). The integration led us to a steady pulse with phase $\pi/2$ for the final state (not shown). In other words, one ends up with steady-state $q=+1$ pulse corresponding to this new $\tilde{\alpha}$. We now turn to the stability of the pulses shown in Fig. 4. In this case, $q=-1$ pulse turns out to be the stable one with both the phases asymptotically reaching the value zero. These results are shown in Fig. 8.

In order to see whether the above-mentioned pulsed solutions are the only steady-state solutions of the system, we look for other solutions of Eqs. (4.2)–(4.4) sub-

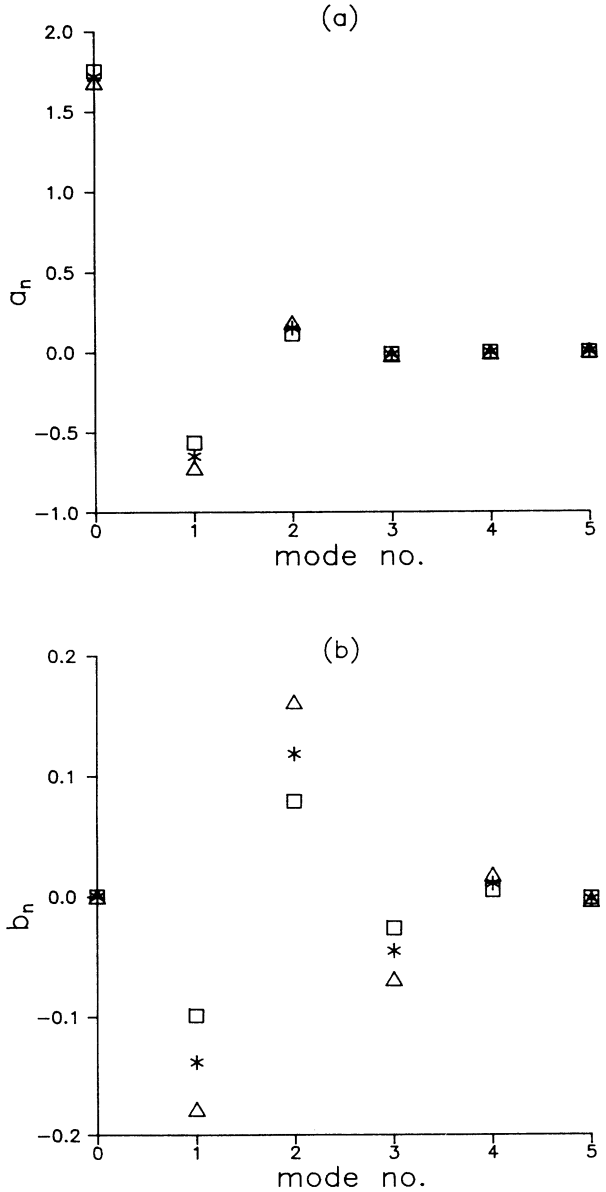

FIG. 6. Mode contents of the steady-state electric field given in Fig. 4(a): (a) cosine component a_n and (b) sine component b_n. The asterisks correspond to the RN pulse whereas the triangles (squares) refer to $q=-1$ ($q=+1$) and $\tilde{g}/\tilde{\kappa}=0.04$.

ject to the boundary conditions given in Eq. (4.7). In other words, we address the question of uniqueness of the nonlinear boundary value problem with unknown parameter $\tilde{\epsilon}$. To answer this question we tried various initial guesses for $e(0)$, $\sigma(0)$, and $\tilde{\epsilon}$. We ended up with a solution which is quite distinct from the ones discussed above. These results are shown in Fig. 9. We have reproduced the RN pulse in Fig. 9(d) for comparision. These solutions with or without the PA are characterized by larger velocities and smaller amplitudes. We investigated the stability of these pulses. They turn out to be unstable. However, the existence of these steady-state solutions suggests that the solution of the problems posed above is not unique. There may be other steady-state solutions which might turn out to be stable. Moreover, one may search for mechanisms that render the solutions of Fig. 9 stable. This may eventually lead to a bistable operation between pulsed states.

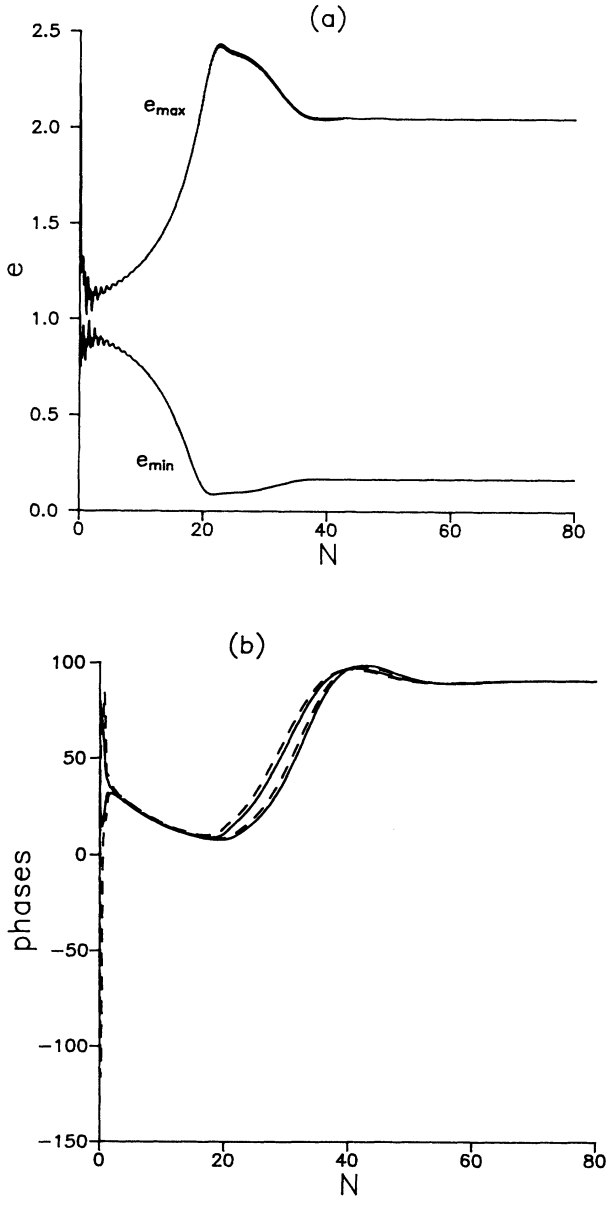

FIG. 7. Temporal evolution of (a) maximum and minimum electric fields e_{max}, e_{min} and (b) maximum and minimum phases of the electric field ϕ_{max}, ϕ_{min} (solid lines) and polarization ψ_{max}, ψ_{min} (dashed lines) as solutions of the set of Eqs. (2.7)–(2.11). The initial values were chosen as $e = e_s + i$, $p = p_s$, $\sigma = \sigma_s$, where e_s, p_s, σ_s correspond to the curves with smaller dashes in Fig. 3. The value of $\tilde{\kappa}$ was chosen to be 1.3. N along the horizontal axis gives the number of round trips in time t, i.e., $N = t/(L/v)$.

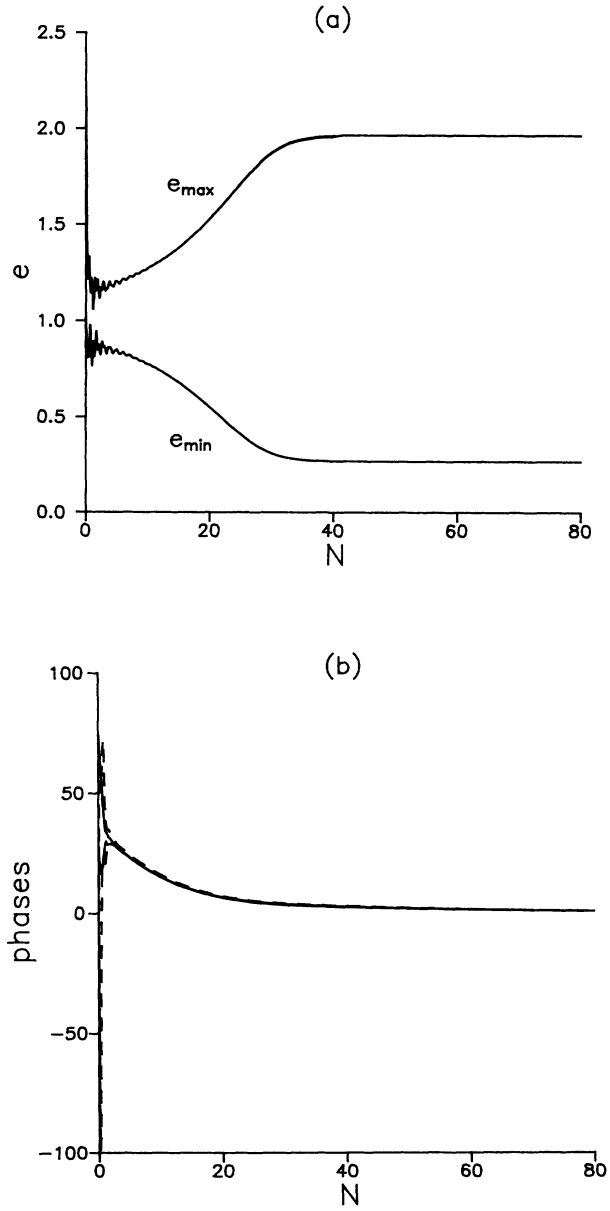

FIG. 8. Same as in Fig. 7 except that now e_s, p_s, σ_s correspond to the curves with larger dashes in Fig. 4.

V. CONCLUSIONS

In conclusion, we investigated a homogeneously broadened two-level ring laser with a $\chi^{(2)}$ material inside the cavity. We calculated the cw states of the system and investigated their linear stability. We showed that in contrast to the case where the $\chi^{(2)}$ material is absent one now has two second thresholds for the amplitude instability of these modes. We also studied the steady-state pulsed solutions of the system and showed that two types of pulses are possible. Our calculations suggest that one can manipulate the pulse width with the intracavity parametric amplifier. We presented some preliminary results on the stability of these pulses. The results suggest that the coexistence of these two pulsed solutions is not possi-

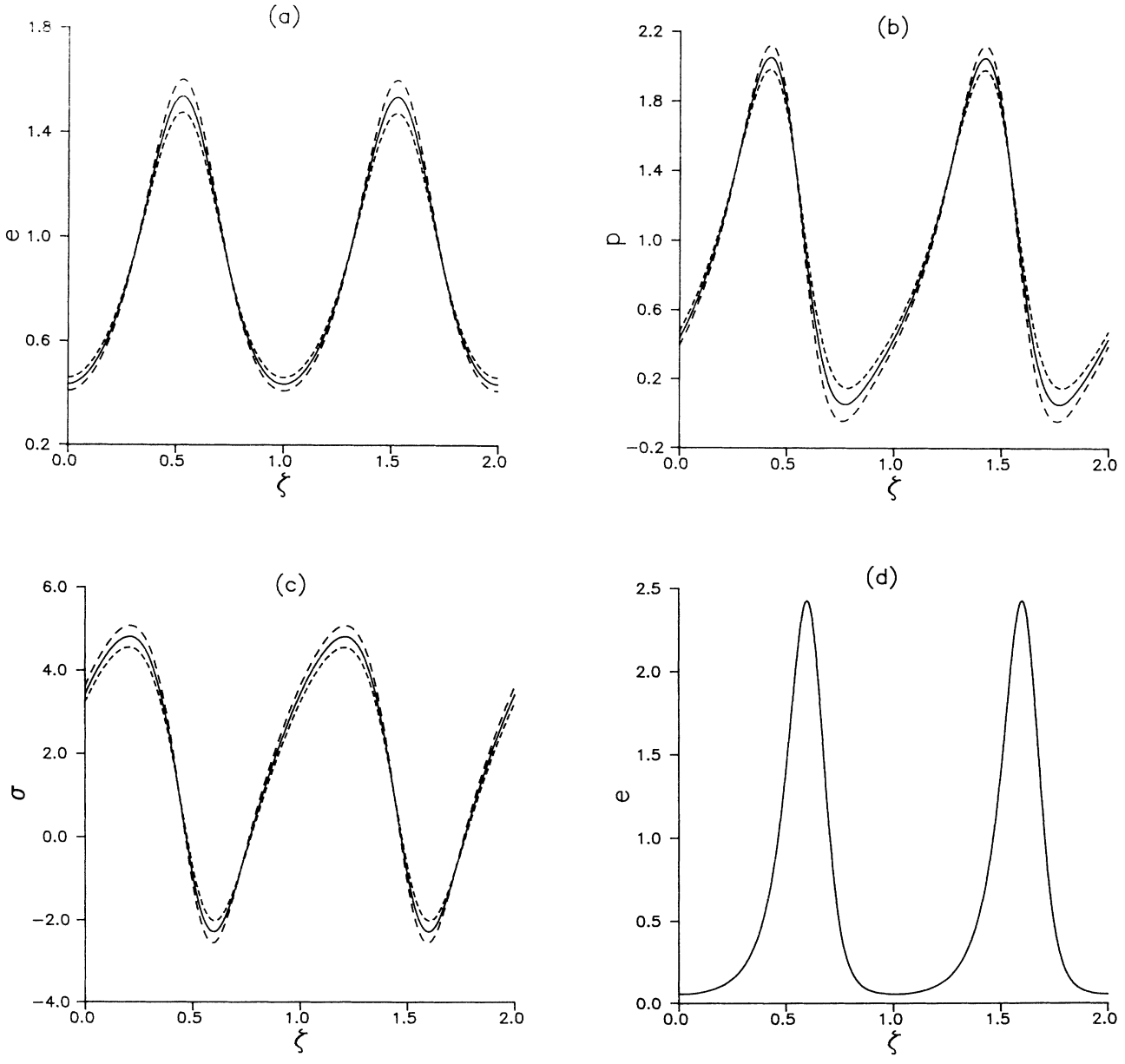

FIG. 9. Steady-state solutions (a) e, (b) p, and (c) σ as functions of ζ with (dashed curves) and without (solid curves) the PA for $\bar{\alpha}'=2.7$. Curves with smaller (larger) dashes correspond to $q=+1$, $\bar{g}/\bar{\kappa}=0.04$ ($q=-1$, $\bar{g}/\bar{\kappa}=0.04$). (d) The RN pulse (with $g=0$) corresponding to the same set of parameters. Other parameters are $\lambda=15$, $\gamma_{\parallel}=0.5$.

ble for specific system parameters. A detailed analysis of the stability of these pulses is underway and is planned to be published elsewhere. Finally we showed that the Risken-Nummedal pulses are not the only pulsed solutions of the steady-state equations and there may be other kinds of solutions. We found one such solution, which, however, turns out to be unstable.

ACKNOWLEDGMENTS

The authors would like to thank the Council of Scientific and Industrial Research, Government of India, for supporting this work. One of the authors (S.D.G.) is grateful to G.S. Agarwal and H. Risken for helpful suggestions.

[1] S. Dutta Gupta and G. S. Agarwal, J. Opt Soc. Am. B **8**, 1712 (1991).

[2] M. B. Pande and S. Dutta Gupta, J. Mod. Opt. **39**, 1643 (1992).

[3] B. H. W. Hendricks, M. A. M. de Jong, and G. Nienhuis, Opt. Commun. **77**, 435 (1990).

[4] For a review of instabilities and chaos in lasers, see, for example, J. R. Ackerhalt, P. W. Milonni, and M. L. Shih, Phys. Rep. **128**, 205 (1985); L. W. Casperson, in *Optical Instabilities,* edited by R. W. Boyd and M. G. Raymer (Cambridge University Press, Cambridge, 1986), p. 58; N. B. Abraham, *ibid.,* p. 46; F. T. Arecchi, *ibid.,* p. 183; L. A. Lugiato and L. M. Narducci, *ibid.,* p. 34; J. Opt. Soc. Am. B **2**, 7 (1985).

[5] For a standard analysis of the single- and multimode laser operation see, for example, H. Haken, *Laser Theory* (Springer, Berlin, 1984).

[6] cw instability of off-resonance modes was reported in H. Risken and K. Nummedal, Phys. Lett. **26A**, 275 (1968).

[7] H. Risken and K. Nummedal, J. Appl. Phys. **39**, 4662 (1968).

[8] For periodic and chaotic breathing pulse solutions see M. Mayr, H. Risken, and H. D. Vollmer, Opt. Commun. **36**, 480 (1981).

[9] For analytic solution of PDE's (in the absence of the PA) for λ close to the critical value, see, H. Haken and H. Ohno, Opt. Commun. **16**, 205 (1976). See also H. Haken, *Synergetics— An Introduction* (Springer, Berlin, 1977), pp. 239–244.